

Quantitative Analysis of Phases in Zeolite Bearing Rocks from Full X-ray Diffraction Profiles*

J. C. Taylor^A and *S. R. Pecover*^B

^A Division of Energy Chemistry, CSIRO, Lucas Heights Research Laboratories, Private Mail Bag 7, Menai, N.S.W. 2234, Australia.

^B Geological Survey of New South Wales, Department of Mineral Resources, 8-18 Bent Street, Sydney, N.S.W. 2000, Australia.

Abstract

It is shown that quantitative analysis of zeolite phases in mineral mixtures can be performed using calculated whole-pattern X-ray diffraction profiles and Bragg-Brentano patterns. The method was tested on binary and ternary standard mixtures containing quartz, heulandite, chabazite and stellerite, and gave zeolite weight percentages correct to within a few per cent. Structure analyses of the zeolites were necessary to obtain good calculated profiles. The platy zeolites heulandite and stellerite had severe preferred orientation problems, which were minimised experimentally by adding Al powder diluent and an epoxy resin, and regrinding. Analyses of field samples are also described.

1. Introduction

Natural zeolites are crystalline, hydrated alumino-silicates containing alkali and alkaline earth cations in an infinite three-dimensional crystal framework. There are over forty-five distinct species of natural zeolites and they occur in rocks of diverse age, type and geological setting. Once thought to be confined mainly to cavities in rocks such as basalts, natural zeolites are now known to occur as major constituents of many bedded volcanic fragmentary rocks and in slightly metamorphosed rocks. In these rocks they generally occur as micron to submicron size crystals intermixed with a variety of other silicate phases. The cation exchange, adsorption and molecular sieving properties of zeolites allow them to be used in a wide variety of industrial and agricultural applications (for example in water purification, soil conditioning, stock feeds and odour control reagents). Large deposits are currently being exploited in Japan, the United States and the Soviet Union.

At present there is considerable exploration interest in zeolite bearing rocks occurring in parts of New South Wales, Australia. However, as with zeolite bearing rocks found elsewhere in the world, successful development of these resources is heavily dependent upon good zeolite characterisation. One of the most important characterisation requirements for zeolite exploration and product development is an accurate determination of the type and amount of zeolite minerals and other phases contained in prospective rocks. Likely rock types for zeolite minerals are those which have been formed by volcanic processes and which contained a high vitric component at the time of deposition. Volcanic glasses of predominantly acid to intermediate composition are the most common starting materials for the formation

* Paper presented at the International Symposium on X-ray Powder Diffractometry, held at Fremantle, Australia, 20-23 August 1987.

of zeolites. The development of zeolites in these rocks is influenced by a variety of physio-chemical conditions, including the original composition of the starting materials, the composition of reaction pore waters moving through the rock, the activities of various competing ions in solution, the partial pressure of H₂O and the temperature and load pressures. However, not all the volcanic glass in a given mass of volcanic ash will alter to zeolite phases. Commonly, zeolite minerals form discrete zones, while in other parts of the rock mass volcanic glass may alter to a combination of quartz, feldspar, chlorite, and/or clay minerals under differing physio-chemical conditions. Furthermore, some zones may develop in which there is a combination of zeolitic and non-zeolitic phases. In the field these differences in mineral type and content are very difficult to detect, particularly if the rock is fine-grained. In order to overcome the problem of determining which rocks are zeolitic and which are not, it is necessary to carefully collect many closely spaced samples across suspected zeolitic and non-zeolitic zones, for the purposes of X-ray diffraction analysis. However, until recently X-ray diffraction analysis of zeolitic rocks provided at best only a semi-quantitative breakdown of the phases present in these rocks, which often resulted in prospective deposits being either overlooked or overrated.

The only techniques capable of determining phase content, as opposed to elemental content, are diffraction methods. Neutron diffraction, with its low specimen neutron absorption and large sample volumes is potentially the best technique, but thermal neutron sources are few and expensive, and we are therefore generally left with the X-ray method.

Until recently, X-ray quantitative analysis has been a rather uncertain procedure, with analysis confined to regions of the pattern with resolved lines, and reliance on standard calibration mixtures. There are also, for unfavourable non-spherical morphology, severe problems with preferred orientation. Complications can also occur with amorphous content, and different channel contents of the zeolites in different locations.

It is inconvenient to make up calibration standards for every possible case. A better approach is to use calculated profiles which are free from the orientation effects. Full-profile procedures have recently been invoked using calculated or standard patterns (Werner *et al.* 1979; Weiss *et al.* 1983; Toraya *et al.* 1984; Smith *et al.* 1986; Hill and Howard 1987). With calculated patterns, multiphase modification of the Rietveld (1969) profile refinement procedure can be used.

Instead of choosing mineral systems with simple structures, which are known to be relatively free of orientation effects and compositional variations, we choose to study here zeolite minerals, because of their industrial importance. Although the zeolites have (Si, Al)O₂ frameworks of fixed geometry for a particular family, the channel contents can vary with location. Also, the platy zeolites studied here, heulandite and stellerite, have severe orientation problems. It is of interest to see how well X-ray quantitative analysis profile methods can perform with standard Bragg-Brentano geometry (whose flat-sample preparation enhances the orientation problems and is prone to instrumental aberration) under these 'worst-possible case' conditions.

2. Method

A computer program for structural analysis of powder patterns by profile-fitting has been described elsewhere (Taylor *et al.* 1986). Extracted (*hkl*) intensity data are

derived by decomposition of the profile and the program SHELX (Sheldrick 1976) is used for the structural refinement. The process is two-stage, in contrast with the one-stage Rietveld (1969) procedure. The program has been adapted for quantitative analysis by allowing for successive pattern subtraction. SHELX outputs $F(hkl)$ on the absolute scale for the theoretical zeolite structure, correct (hkl) multiplicities are attached and the profile scale factor is varied graphically until the calculated pattern matches in intensity with its mate in the observed pattern. All phases in the mixture are removed in this way until the residual pattern is as close to zero as possible. The usual instrumental parameters (Rietveld 1969) are used. They are usually entered by inspection (multiphase refinement can give parameter correlation), but can be varied by least-squares by stripping the pattern to a particular phase. It is particularly important to have a good value of the half-width parameters. Calculated structures can also be refined by stripping to one phase and using the two-stage refinement process. One should have a good standard model for a calculated phase, but even if the model is not perfect, the deviations between observed and calculated patterns 'average out' about the zero line over the whole pattern, and the effect on the scale factor may not be serious.

The program has a preferred orientation correction of the Rietveld type, but this should only be used for structure analysis. In quantitative analysis, the fact that all intensity corrections with $\exp(-G\alpha^2)$ (see Rietveld 1969 for an explanation of the symbols) are in the one direction destroys the meaning of the scale factor. We have chosen to reduce the preferred orientation effect experimentally by adding Al powder diluent and regrinding after mixing with an epoxy resin (5-minute Araldite). This greatly reduces the particle orientation without any obvious effect on the zeolite structure. The first aluminium line at $2\theta = 45^\circ$ is past the region of interference for the zeolites, as they have many strong lines in the profile below this angle which can be used. The price paid for adding the diluents is a two-thirds drop in intensity. It was found, however, that it was impossible to analyse the mixtures until the orientation was reduced with diluents. Even though the orientation was never completely removed its effect was reduced, allowing the scale factors to be determined by graphically 'averaging out' over the now smaller orientation-induced fluctuations in the observed pattern.

The most noticeable orientation effect in the heulandite and stellerite patterns was the enhancement of the basal reflection at $\approx 11^\circ 2\theta$ (see Figs 2-5, 7 and 8 below). On the other hand, quartz and chabazite, the other model phases with roughly spherical crystallites, showed little orientation.

A further problem with zeolites is that their channel contents vary with location. Thus, the chabazite structures of Alberti *et al.* (1982) and Calligaris *et al.* (1982) were found to give calculated powder patterns which did not agree in intensity with a pattern measured for pure Tambar Springs (N.S.W.) chabazite. The structural parameters for the Australian chabazite including channel contents were therefore determined for the Australian mineral by two-stage profile refinement; this was the model for our calculated chabazite patterns used for analysing the N.S.W. zeolites.

The structural models for Australian heulandite and stellerite were determined on single-crystal specimens from the Tambar Springs area by neutron diffraction (Hambley and Taylor 1984; Miller and Taylor 1985); these are the models used for the calculated heulandite and stellerite patterns. Quartz and chabazite parameters used were from analysis of X-ray patterns of samples taken from the same area.

The mass percentages were calculated with the formula of Hill and Howard (1987) as the product of the scale factor, mass, and volume of the unit cell.

3. Experimental

X-ray diffractometer patterns were collected for five heulandite–quartz mixtures: two ternary quartz–chabazite–stellerite mixtures, chabazite, stellerite and quartz from the Tambar Springs (N.S.W.) area with and without diluents. Conditions of collection were: Co K α radiation ($\lambda = 1.7902 \text{ \AA}$), 0.05° steps, post-diffraction graphite monochromator, 1° divergence slit and scintillation detector. The samples were finely ground. Corrections were made for the effects of monochromator polarisation, sample irradiation area and divergence of the beam past the sample at low angles.

The fine grinding and diluent addition did not appear to change the zeolite patterns significantly, except to reduce the orientation, and make the observed patterns closer to the theoretical ones.

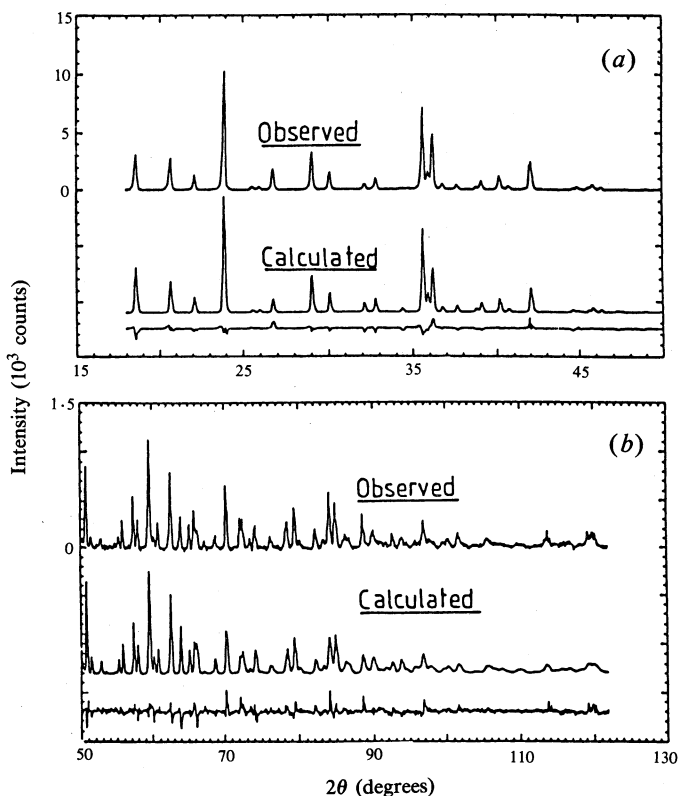


Fig. 1. Results of structural refinement of Tambar Springs chabazite showing observed and calculated X-ray powder profiles for 2θ in the range (a) 18° – 50° and (b) 50° – 122° .

4. Results

(a) Refinement of Quartz and Chabazite Structures for Tambar Springs Specimens

Quartz. Quartz crystals growing on a piece of stellerite from Tambar Springs were ground and an X-ray powder pattern collected to $2\theta = 110^\circ$. Starting with structural data from Wyckoff (1964), profile refinement converged to

$$R(\text{profile}) = \Sigma(|y_b| - |y_c|) / \Sigma |y_b| = 0.17,$$

$$R(\text{Bragg}) = \Sigma(|F_0| - |F_c|) / \Sigma |F_0| = 0.08.$$

The results were as follows: $u(\text{Si}) = 0.469(2)$, $x(\text{O}) = 0.417(4)$, $y(\text{O}) = 0.272(4)$, $z(\text{O}) = 0.120(3)$, $a = 4.9146(1) \text{ \AA}$, $c = 5.4036(2) \text{ \AA}$. The isotropic thermal parameters were $U(\text{Si}) = 0.010(4) \text{ \AA}^2$ and $U(\text{O}) = 0.023(6) \text{ \AA}^2$. The instrumental half-width parameters were $U = 0.05(1)$, $V = -0.05(1)$ and $W = 0.029(1)$ (the symbols are explained in Rietveld 1969). The quartz parameters were not appreciably different from literature values, so the quartz was reasonably pure.

Chabazite. Chabazite crystals of twinned phacolithic habit were found growing on a rock from Tambar Springs with stellerite and laumontite. Some crystals were prised

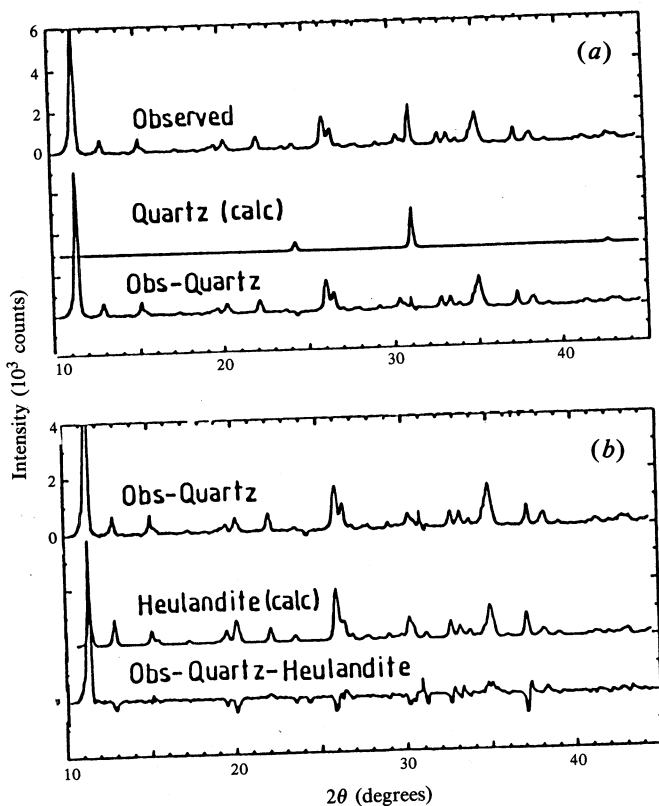


Fig. 2. Quantitative analysis of 85% heulandite, 15% quartz mixture showing (a) quartz subtraction and (b) heulandite subtraction.

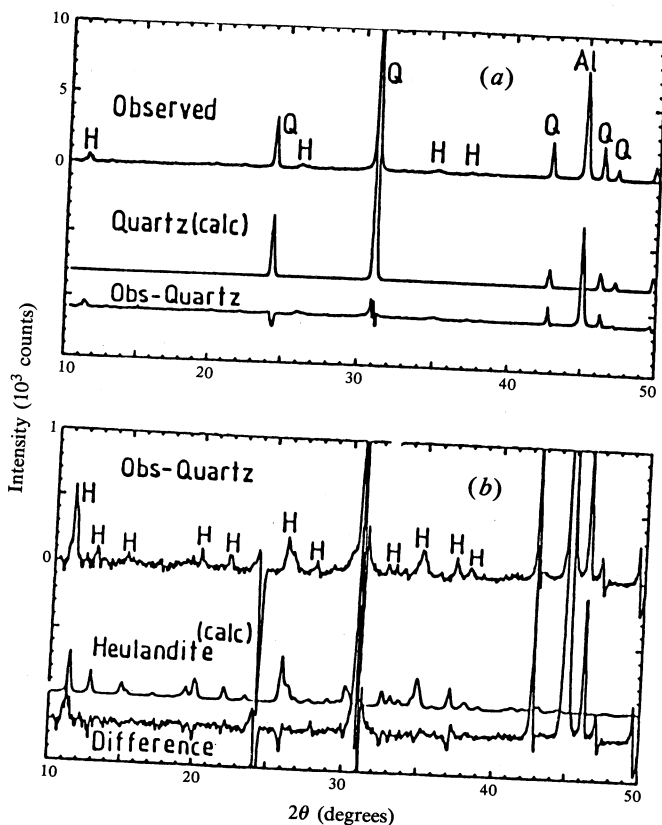


Fig. 3. Quantitative analysis of 14% heulandite, 86% quartz mixture showing (a) quartz subtraction and (b) heulandite subtraction.

off, ground and an X-ray diffraction pattern taken. As the intensities were different from those calculated from the data of Alberti *et al.* (1982) and Calligaris *et al.* (1982) a structural analysis was attempted with the X-ray data, using Fourier analysis to locate channel atoms. At the present stage of refinement, the profile R -factor is 0.24 and the $R(\text{Bragg})$ is 0.09, which is sufficient for the present quantitative analysis study. The twinning causes minimal preferred orientation. The space group was taken as $R\bar{3}m$, although the refined cell dimensions suggested a small triclinic deviation, which has been noted previously (Gottardi and Galli 1985). The rhombohedral cell refinement gave $a = 9.386(1) \text{ \AA}$ and $\alpha = 94.436(5)^\circ$, and the cell, assuming triclinic symmetry, was $a = 9.385(1) \text{ \AA}$, $b = 9.394(1) \text{ \AA}$, $c = 9.392(2) \text{ \AA}$ and $\alpha = 94.392(4)^\circ$, $\beta = 94.475(5)^\circ$, $\gamma = 94.404(8)^\circ$.

The observed and calculated profiles for the Tambar Springs chabazite are given in Fig. 1.

(b) Quantitative Analysis of the Binary Heulandite-Quartz Mixtures

The analyses of the heulandite-quartz mixtures are illustrated in Figs 2 and 3 for the 85:15% and 14:86% mixtures. The quartz subtractions, being straightforward, are done first. In the heulandite subtractions the first heulandite peak at $11.5^\circ 2\theta$ is ignored as it is the plate reflection, enhanced by preferred orientation. The low-angle

data are also less reliable because of the beam-divergence effect. Fig. 2 shows that preferred orientation of the crystals is not completely eliminated by the Al powder and resin, as shown by the enhancement of the plate reflection at 11.5° , but over the pattern the observed and calculated profiles for heulandite match reasonably well. Before addition of the diluent, the observed pattern was completely unrecognisable as heulandite, and quantitative analysis was impossible. Scale factors were estimated for quartz and heulandite graphically. It is seen that as the quartz content increases, the quartz residuals at 24° and 31° become more significant, but do not affect the scale factor estimate for heulandite over the rest of the pattern.

On first inspection, the pattern for 14% heulandite, 86% quartz in Fig. 3a appears to have no heulandite peaks. However, on expanding the y -scale of the (observed—quartz) pattern (see Fig. 3b), weaker peaks are seen (labelled H) which match well the calculated pattern of heulandite, and a quantitative analysis with the H peaks is thus possible. Even at this low heulandite concentration, and with the addition of the diluents, preferred orientation of the heulandite is not removed, as the plate reflection at $11.5^\circ 2\theta$ is still enhanced.

The above analyses would not have been possible without the sample diluents. The Rietveld (1969) preferred orientation correction, while being a convenient factor for structure refinement, does not conserve intensity; thus we reduce the orientation experimentally as shown.

Table 1. X-ray quantitative analysis of binary quartz–heulandite mixtures

Unit cell mass and unit cell volume for quartz and Garrawilla heulandite are 180 a.m.u., 113.0 \AA^3 and 2750 a.m.u., 2123 \AA^3 respectively

Phase	Profile scale	$W(\text{phase})^A$	Wt% found	Wt% actual
Heulandite	0.000016	94.4	12.7	13.7
Quartz	0.0315	640.7	87.3	86.3
Heulandite	0.000055	321.1	28.8	27.7
Quartz	0.0390	793.3	71.2	72.3
Heulandite	0.000065	379.5	45.0	49.4
Quartz	0.0228	463.8	55.0	50.6
Heulandite	0.000070	408.7	65.0	67.0
Quartz	0.0108	219.6	35.0	33.0
Heulandite	0.000082	478.7	88.3	84.6
Quartz	0.00313	63.7	11.7	15.4

^A Product of the profile scale, the mass of the unit cell, and the unit cell volume.

The results for the binary mixtures are given in Table 1. It can be seen that the method gives mass percentages to within a few per cent. In favourable cases with no orientation it should be possible to estimate the percentages to less than one per cent (with no amorphous content).

(c) Quantitative Analysis of Ternary Quartz–Chabazite–Stellerite Mixtures

Fig. 4 illustrates the analysis of a quartz–chabazite–stellerite mixture, called Q–C–S mixture 1, with the as-mixed and ground sample (no orientation-reducing diluents). The quartz and chabazite subtractions are shown in Figs 4a and 4b. However, severe

problems are encountered (see Fig. 4c) in matching the calculated and observed intensities for the oriented stellerite. The mismatch is such that the stellerite scale cannot be estimated, so here only the quartz-chabazite ratio can be found.

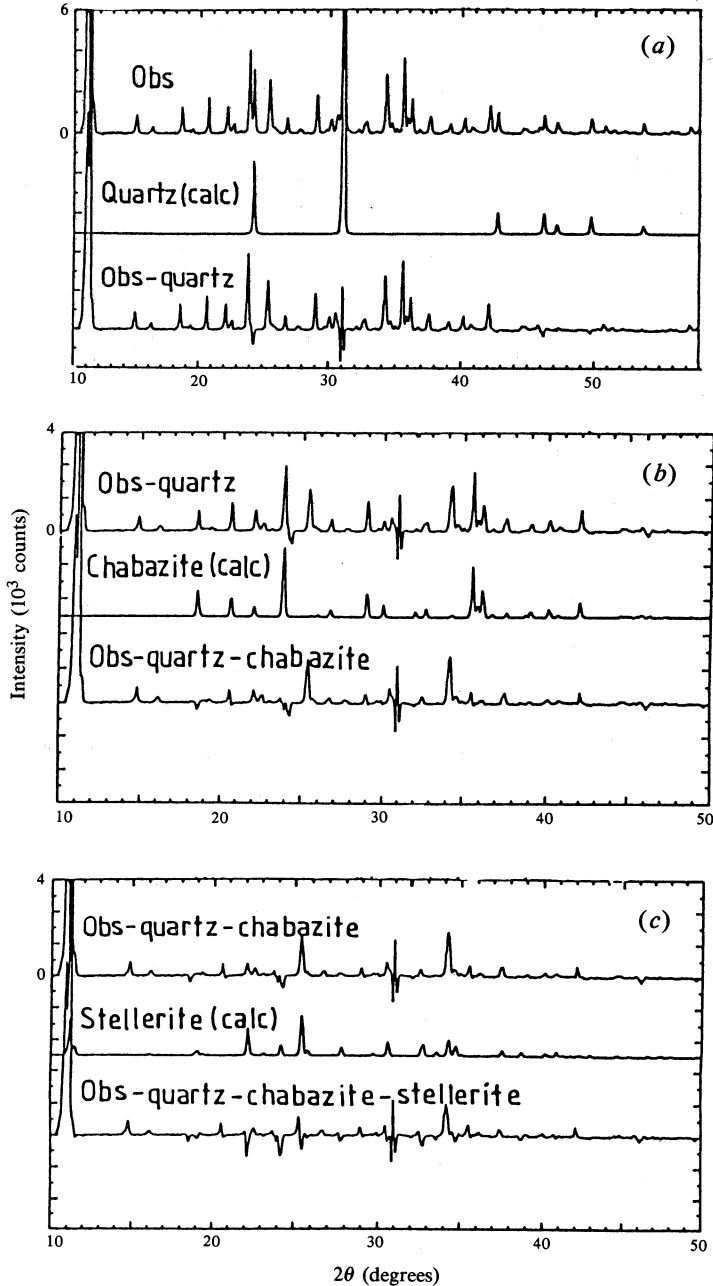


Fig. 4. Quantitative analysis of quartz-chabazite-stellerite mixture 1 showing (a) quartz subtraction, (b) chabazite subtraction and (c) stellerite subtraction. In this case no Al powder or epoxy resin has been added to reduce preferred orientation of the stellerite.

Fig. 5 illustrates the analysis when Al and resin are added. In Fig. 5c it is seen that now the stellerite patterns match reasonably well and the scale factor for the stellerite pattern can be estimated. The peaks at 15° and 29° are chabazite residuals, while the noise at 24° and 31° is due to an imperfect quartz subtraction. In Fig. 5, the first Al peaks at 45° and 52° have been removed and replaced by the background level, for clarity.

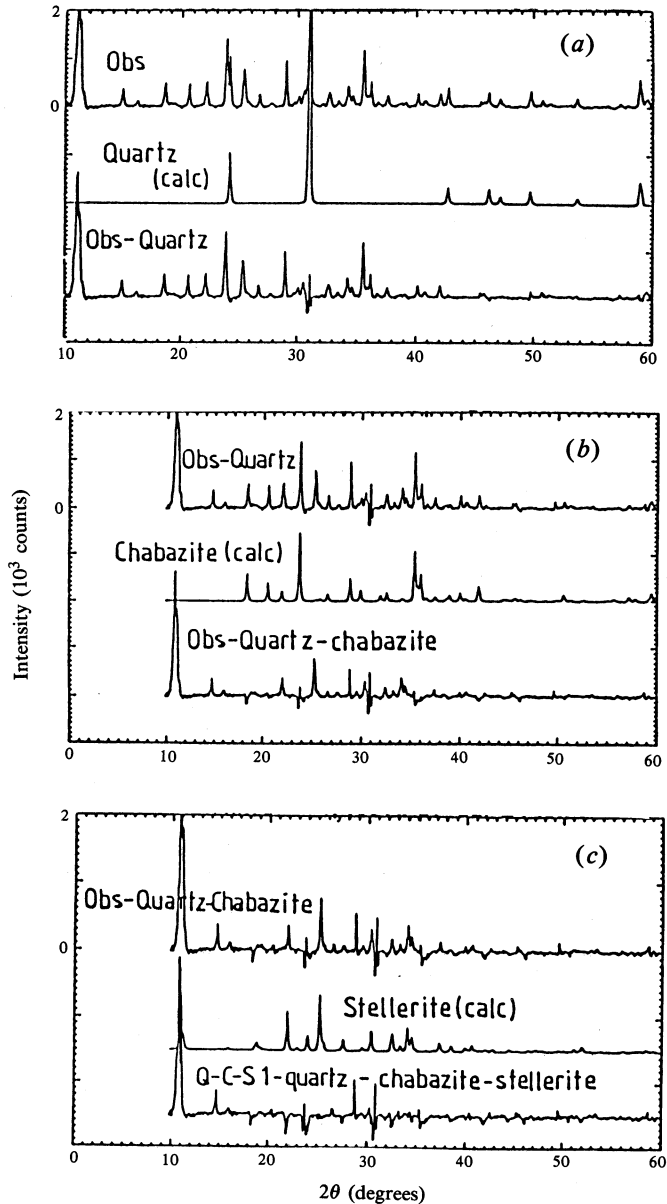


Fig. 5. Quantitative analysis of quartz-chabazite-stellerite mixture 1 showing (a) quartz subtraction, (b) chabazite subtraction and (c) stellerite subtraction. Here the stellerite crystallite preferred orientation has been reduced by addition of Al powder and epoxy resin.

Table 2. Quantitative analysis of ternary quartz–chabazite–stellerite mixtures

Unit cell mass and unit cell volume are as follows: quartz 180 a.m.u., 113 Å³; Garrawilla chabazite 1030.7 a.m.u., 831 Å³; Garrawilla stellerite 5524 a.m.u., 4403 Å³

Phase	Profile scale	<i>W</i> (phase)	Wt% phase (calculated)	Wt% phase (actual)
<i>(a) Q–C–S mixture 1</i>				
Quartz	0.0080	162.7	31.0	30.7
Chabazite	0.000286	245.0	46.7	42.8
Stellerite	0.00000485	116.7	22.3	26.5
<i>(b) Q–C–S mixture 2</i>				
Quartz	0.0112	227.7	23.9	23.9
Chabazite	0.00045	385.4	40.4	41.8
Stellerite	0.000014	340.5	35.7	34.3

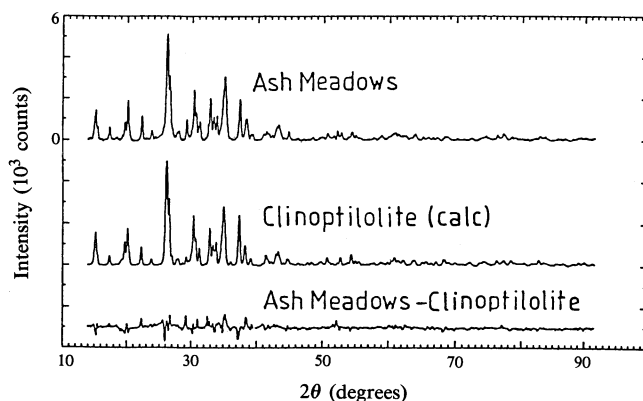


Fig. 6. Analysis of Ash Meadows (U.S.A.) natural zeolite. The observed pattern is matched well by the calculated pattern from the Alberti (1975) structural model.

A second quartz–chabazite–stellerite mixture, Q–C–S mixture 2, was analysed in a similar way. The results for the ternary mixtures (a) Q–C–S(1) and (b) Q–C–S(2) are given in Table 2.

It is seen that again the mass percentages of the three phases present are reliable to within a few per cent. The discrepancies between actual and determined amounts are due mainly to the stellerite subtraction.

(d) Applications to Field Samples

We choose two U.S.A. zeolite samples with minerals similar to those in the standard mixtures as examples. Work has also commenced on a suite of fine-grained zeolites from the Eagleton quarry, near Raymond Terrace, N.S.W.

Ash Meadows Zeolite (California/ Nevada, U.S.A.). This sample analyses as 100% clinoptilolite (excluding amorphous content). Clinoptilolite is a zeolite of the heulandite family, with a similar framework and powder pattern to heulandite. Fig. 6

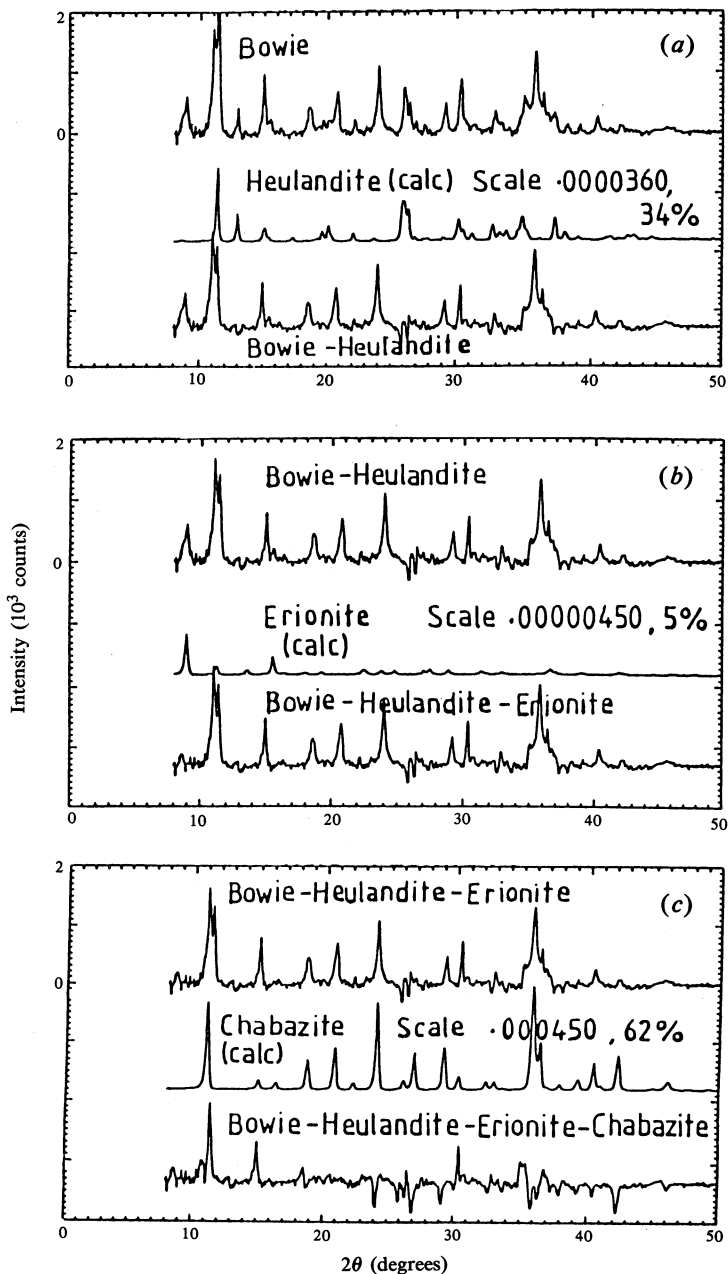


Fig. 7. Quantitative analysis of Bowie (U.S.A.) natural zeolite showing (a) heulandite subtraction, (b) erionite subtraction and (c) chabazite subtraction.

shows the Ash Meadows pattern from $14^\circ 2\theta$ upwards and a pattern calculated from the structural data of Alberti (1975) (the Alberti parameters have not been refined). It is apparent from the difference pattern that there are only slight differences between the Ash Meadows clinoptilolite structure and the model of Alberti.

Bowie Zeolite (Arizona, U.S.A.). The analysis is illustrated in Fig. 7. The peaks at 11.5° and 26° suggest a zeolite of the heulandite–clinoptilolite family. Fig. 7a shows the subtraction of a heulandite pattern. The peak at $9^\circ 2\theta$ can be attributed to the zeolite erionite, and Fig. 7b shows the erionite subtraction. The other erionite peaks are very small. There is a large chabazite content, but we deferred its subtraction because the chabazite intensities differ from literature models due to a variation in channel content. Fig. 7c shows the chabazite subtraction. The final residuals are now nearly all at chabazite angles, except at 11.5° , the angles of the heulandite plate reflection. The chabazite scale is chosen to average chabazite residuals to zero. The actual chabazite structure could possibly be refined with the pattern in Fig. 7c. The scale factors chosen give 61.7% chabazite, 33.6% heulandite or clinoptilolite and 4.7% erionite, excluding possible amorphous content.

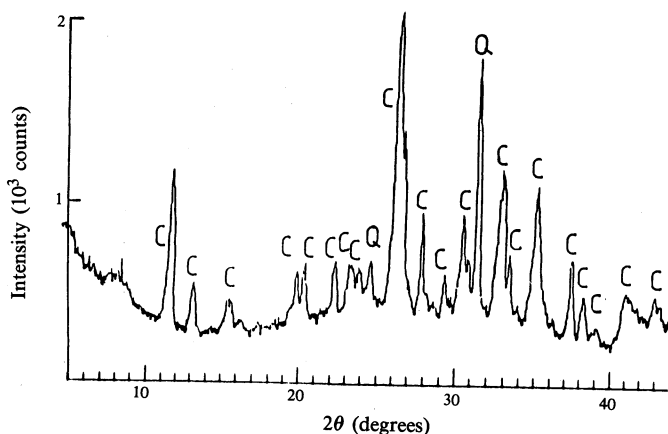


Fig. 8. X-ray diffraction pattern of Eagleton Quarry (N.S.W.) natural zeolite, showing the zeolite clinoptilolite (C) and quartz (Q) lines.

Eagleton Quarry (N.S.W.). Eagleton zeolite is of the clinoptilolite family, and occurs with quartz. Fig. 8 shows the X-ray pattern including background of an Eagleton sample which is essentially clinoptilolite (C) and quartz (Q). Addition of the orientation-reducing resin causes the high curving background, and some loss in intensity. The zeolite mass fraction is about 87%.

5. Conclusions

The above work suggests that it should be possible to estimate mass percentages of different zeolites in zeolitic materials to within 1% if preferred orientation is completely removed, either experimentally or by using an intensity-conserving theoretical correction, such as that given by Dollase (1986). Preferred orientation corrections of the type given by Rietveld (1969) should be avoided. In actual samples, with reduction of orientation by the above method, the percentages are correct to within a few per cent. If amorphous content is suspected, it can be estimated by adding a known weight percentage of a standard such as corundum. Small deficiencies in calculated structural models are not serious, because we average out residuals over the pattern to zero. These results are encouraging as we have chosen some very complex structures and crystallites which orient strongly. The

technique will be used to determine the zeolite type and content of fine-grained volcanic ash deposits in some areas of New South Wales which are currently under investigation by exploration companies, and in checking the efficiency of separation processes for upgrading coarse-grained zeolitic rocks such as chabazite, heulandite, and stellerite-bearing basalts.

Acknowledgments

We wish to thank Dr C. J. Ball for the use of a diffractometer and Dr C. J. Howard for a preprint and discussion. We thank CSIRO and the Department of Mineral Resources for their permission to publish this paper.

References

- Alberti, A. (1975). *Tschermaks Min. Petr. Mitt.* **22**, 25–37.
- Alberti, A., Galli, E., Vezzalini, G., Passaglia, E., and Zanazzi, P. (1982). *Zeolites* **2**, 303–9.
- Calligaris, M., Nardin, G., Randaccio, L., and Chiaramonti, P. (1982). *Acta Crystallogr. B* **38**, 602–5.
- Dollase, W. A. (1986). *J. Appl. Crystallogr.* **19**, 267–72.
- Gottardi, G., and Galli, E. (1985). 'Natural Zeolites', p. 175 (Springer: Berlin).
- Hambley, T. W., and Taylor, J. C. (1984). *J. Solid State Chem.* **54**, 1–9.
- Hill, R. J., and Howard, C. J. (1987). *J. Appl. Crystallogr.* (in press).
- Miller, S. A., and Taylor, J. C. (1985). *Zeolites* **5**, 7–10.
- Rietveld, H. M. (1969). *J. Appl. Crystallogr.* **2**, 65–71.
- Sheldrick, G. M. (1976). SHELX-76 program system. University of Cambridge.
- Smith, D. K., Johnson, G. G., and Ruud, C. O. (1986). *Adv. X-ray Anal.* **29**, 217–24.
- Taylor, J. C., Miller, S. A., and Bibby, D. M. (1986). *Z. Kristallogr.* **176**, 183–92.
- Toraya, H., Yoshimura, M., and Somiya, S. (1984). *Commun. Am. Ceramic Soc.* C119–21.
- Weiss, Z., Krajicek, J., Smrcok, L., and Fiala, J. (1983). *J. Appl. Crystallogr.* **16**, 493–7.
- Werner, P. E., Salome, S., Malmros, G., and Thomas, J. O. (1979). *J. Appl. Crystallogr.* **12**, 107–9.
- Wyckoff, R. W. G. (1964). 'Crystal Structures', Second edition (Wiley Interscience: New York).

